RSC Advances

ROYAL SOCIETY OF CHEMISTRY

www.rsc.org/advances

Spectroscopic signatures and structural motifs in isolated and hydrated theophylline: a computational study

Vipin Bahadur Singh*
Department of Physics, Udai Pratap Autonomous College, Varanasi-221002, India

Abstract:

The spectra and structures of theophylline monomer and dimer and their hydrated complex have been investigated by MP2 and DFT methods. The ground state geometry optimization yield five lowest energy conformers of Tph_1-$(H_2O)_1$ complex at the M06-2X/6-311++G(d,p) level of theory for the first time. We investigated the low-lying excited states of bare theophylline by means of coupled cluster singles and approximate doubles (CC2) and TDDFT methods and a satisfactory interpretation of the electronic absorption spectra (*Phys. Chem. Chem. Phys.*, 2012,**14**,10677-10682) is obtained. One striking feature is the coexistence of the blue and red shift of the vertical excitation energy of the optically bright state S_1 ($^1\pi\pi^*$) of theophylline upon forming complex with a water at C_2=O and C_6=O carbonyl sites, respectively. The optimized structure of newly characterized theophylline dimer Form IV,computed the first time by MP2 and DFT methods. The binding energy of this dimer linked by double N-H…O=C hydrogen bonds was found to be 88 kj/mole at the MP2/6-311++G(d,p) level of theory. The geometry optimization of dimer Form M has also been performed and found that further stability is being conferred to the dimer IV after hydration. Computed IR spectra is found in remarkable agreement with the experiment (*Cryst. Growth Des.* 2010, **10**, 3879-3886) and the out of phase $(C=O)_2$ stretching mode shows tripling of intensity upon dimerisation. The vertical excitation energy of the optically bright state S_1 ($^1\pi\pi^*$) of theophylline monomer upon forming dimer IV is shifted towards red as well as blue.

Keywords: Anhydrous theophylline dimer Form IV, Ab initio and DFT calculations, Hydrgen binding energy, IR spectra, Hydration, Vertical excitation energies.

---

* **Email: vipinwp_vns@rediffmail.com; Tel: 91-9453762957**

1. Introduction

Theophylline (1, 3-dimethylxanthine) has been one of the most commonly used bronchodilator and respiratory simulator for the treatment of the symptoms of acute and chronic asthmatic conditions for over 70 years.[1] Theophylline, found mainly in tea is known to exist either as anhydrates or a monohydrate.[1-5] The pharmaceutical properties of both the anhydrous and monohydrate material have been studied and shown to differ.[6-9] The anhydrous theophylline had three polymorphs, the stable phase at high temperatures (Form I), the stable phase at room temperature (Form II) and the metastable phase (Form III), and Form II crystals are used as an active pharmaceutical ingredient.[2-4] The crystal structure of form II is characterized by N-H…N hydrogen bonding and two bifurcated C-H…O hydrogen bonds.[3] There was some confusion regarding the (crystal) structural motif and IR spectra of anhydrous theophylline even after almost 50 years of investigation.[10,11]Recently a fourth anhydrous polymorph of theophylline has been characterized and reported by the group of Seton and khammer[10-12] as the most thermodynamically stable form at room temperature. In the reported structure of polymorph form IV, the two theophylline molecules form a dimer via double N-H…O hydrogen bonds.[11,12] Theophylline contains both hydrogen bonded donors (imidazole N-H and C-H) and hydrogen bond acceptors (two carbonyl groups and basic nitrogen). Therefore two types of molecular pairs are most probable, the first pair involving double N-H…O=C intermolecular hydrogen bonds, characterized as a dimer of Form IV [11] and second pair involving one C-H…O and one N-H…N hydrogen bonds, related to anhydrous Form II.[1] N-H..O=C type hydrogen bond plays an important role in biomolecular interactions, such as protein folding and DNA double strand. The dimer arrangement of Form IV is likely to be more thermodynamically stable than the catemar type arrangement of Form II.[12,13]

Spectroscopic signatures of isolated biomolecules and their hydrated clusters may provide insight on their preferred conformations, dynamical flexibility, and inter- and intra- molecular interactions determining their skeletal structures. In the last decade, spectroscopy and photochemistry of nucleic acid bases and related molecular systems have been extensively studied with experimental and theoretical methods.[14-19] A striking feature of the DNA and RNA bases is the efficient deactivation through very fast radiationless decay processes back to the electronic ground state after absorption of UV light which is believed to prevent the bases from destructive photochemical reactions.[14,16] In this regard photo dynamics of nucleic acid analogue,

xanthine (3,7-dihydro-purine-2,6-dione), plays an important role with the goal of transferring the experience obtained in these simpler systems to more complex situation found in DNA. In the gas phase, xanthine and its methyl derivatives can exist in a variety of different tautomeric forms, which can exhibit drastically different photo physical behavior. Resonant two photon ionization (R2PI) experiment performed for the theophylline in the gas phase[18] were all sharp and vibronically resolved, suggesting a long excited state lifetime. Recently, Chen and Kohler[19] experimentally performed the femtosecond transient absorption spectroscopy of the same compound in water and acetonitrile with the same excitation wavelength (266 nm) as used in R2PI spectra[18] and the results suggest, however , that these species relax to the electronic ground state on a subpicosecond time scale. It was shown that the dimer of xanthine had a hydrogen bonded structure, but that the methylated derivatives of xanthine were stacked since the methylation prevented hydrogen bonding.[17] In the gas phase resonant two photon ionization (R2PI) experiments, only theobromine and caffeine dimers were detected, while theophylline dimer was not observed.[18] Possible reasons include unfavorable Franck-Condon Factors, spectral shift, low oscillator strengths, or short excited state life times compared to the nanosecond time scale laser pulses.[18] Few of these effects could play role in the failure to observe hydrogen bonded theophylline dimer by Callahan et al.[18] Unfortunately, while most of the available experimental results have been obtained, none of the computational paper including the stabilization of theophylline dimer Form IV takes into account. The excited states of theophylline are important in understanding photophysics and photochemistry of theophylline-DNA complexes. In the isolated theophylline, the lowest excited state S_1 exhibits $\pi\pi^*$ character and primary photo-excitation involves this optically bright state S_1 ($^1\pi\pi^*$).[17] It is common knowledge that hydration can shift electronic states and hence, it can modify the excited state dynamics. Second order Moller-Plesset perturbation theory (MP2)[20], second order approximate coupled cluster (CC2) [21] and density functional theory (DFT)[22-32,35-37] methods implemented in Gaussian 09[25] and TURBOMOLE 64 [26] quantum chemical software's, provide important insights into the energetic, ground state structures, IR and electronic spectra of these systems. Our aim is to investigate the most stable structural motif and corresponding IR spectra of theophylline monomer and its hydrated and dimeric complexes to verify earlier experimental results. Furthermore, we have computed the vertical excitation energies of the low-lying excited states of theophylline and determined the spectral shift of the lowest singlet $\pi\pi^*$ excited- state upon

forming complex with water and dimer IV. The observed blue shift in the electronic absorption spectra in aqueous solution of theophylline[19] is determined and the possible reason of missing of the dimeric complex in the R2PI spectra[18] will be discussed in view of the earlier experimental and theoretical reports. The effect of hydration on the stability of recently characterized dimer IV is also explored. The application of DFT to non-covalently bound complexes has been limited due to the failure of most density functional approximation, in many case, to describe dispersion interaction. However, several approaches exist for improving existing density functionals to handle dispersion effects. In this paper, we have employed the B3LYP[22-26]and X3LYP[22-26,28] density functionals and newly M06, M06-2X[29-30], wB97X-D[31] and DFT-D3[32] functionals to predict the energy and/or binding energy of theophylline and its monohydrated and dimeric complexes.

2. Computational Methods

Electronic structure calculations have been performed using the Gaussian 09 and Turbomole V6.4 quantum mechanical software packages.[25,26] The ground state of various structural motifs of theophylline were optimized using the second order Moller-Plesset (MP2) perturbation theory [20] and density functional theory employing employing the B3LYP,[22-26] B3PW91,[23-27] X3LYP[22-26,28] and newly developed M06, M06-2X[29-30] and wB97XD[31] exchange-correlation functionals. The ground state structure of the theophylline monomer was also optimized using the resolution of identity (RI) second order approximate coupled cluster (CC2)[21] and the B97-D method using DFT-D3 disperson correction[32] implementations in Turbomole V6.4.[26] For monohydrated theophylline, all possible locations of interactions between theophylline and water were considered, such as oxygen atom in the carbonyl groups, the nitrogen atom, and pi cloud of the ring. The lowest energy conformers were selected from these initial geometries by using the HF method, while their geometry finally optimized by using few of the above methods employed for bare theophylline. Theoretical methods described above were applied to a molecular geometry of theophylline and its hydrated complexes without symmetry restrictions. The calculated geometry with C_1 symmetry was very close to that with C_s symmetry. All optimized structures have been verified as minima by performing frequency calculations in order to ensure that no imaginary frequency were present. In the dimer form IV of theophylline, the molecule has restricted to C_{2h}-symmetry. Four different basis sets were considered: 6-31G (d), 6-31+G(d) and 6-311++ G(d,p),

aug-cc-pVDZ [25,26] for MP2, CC2 and each of DFT functional calculations. Due to the large size, aug-cc-pVDZ basis set could not be used in the optimization of dimer and hydrated complex structures.

B3LYP is known to be a relatively reliable and economical computational method and is extensively employed in the investigation of small and medium sized molecules.[23-28] Marta et al.[33] have reported that there is no significant difference between DFT and MP2 obtained geometries. X3LYP [28](extended hybrid functional with Lee-Yang-Parr correlation functional[23]) extended functional for density functional theory was developed to significantly improve the accuracy for hydrogen bonded and van der waals complexes. The M06 and M06-2X [27,28] are newly developed standard hybrid DFT functionals with parameters optimized on training sets of benchmark interaction energies. Zhao and Truhlar[29-30] developed the hybrid M06 functional that shows promising performance for non covalent interactions. A new DFT method with dispersion correction (DFT-D3) was developed by Grimme and co-workers.[32] The important improvements of the new method[32] are the dispersion coefficients and cut of radii which are less empirical and both computed from first principle. The CC2 method[21] is an approximation to the coupled cluster singles and doubles (CCSD) method where single equations are retained in the original form and the double equations are truncated to the first order in the fluctuating potential.

All harmonic frequencies were scaled in order to compensate the use of a harmonic oscillator approximation in calculating the frequencies, as well as, long range electron correlation effects. Atomic charges were calculated by Natural Bond Orbital (NBO) method embedded in Gaussian 09 software.[25] The binding energies of the dimer Form IV, II and M computed as a difference between the total energy of the complex and the energies of the isolated monomers were further corrected for the basis set superposition error (BSSE) by applying the counterpoise procedure.[34] TD-DFT method[35-37]employing B3LYP functional with 6-311++G(d,p) basis set was used at corresponding (DFT-B3LYP) ground state optimized geometries to predict the electronic absorption wavelengths. RI-CC2 implementation in Turbomole 6.4 employing the basis set 6-311++G(d,p) was also used to compute the vertical excitation energies (VEE) of the theophylline monomer, using CC2/aug-cc-pvdz optimized geometry. The effect due to the so-called bulk water molecules was taken into account within the polarizable continuum model (PCM)[37-38] and the conductor like screening model (COSMO) framework.[38] The electronic absorption spectra in aqueous solution have been calculated by employing the B3LYP hybrid exchange correlation

functionals, using the PCM and COSMO continuum solvent models.[35-39] In this work, the lowest excited $^1\pi\pi^*$ state of theophyllinne was optimized at the TD-B3LYP/6-311++G(d,p) and TD-PBEO[40]/ TZVP levels of theory implemented in Turbomole V6.4.[26]

3. Results and Discussion

3.1. Optimized geometries of theophylline monomer and its hydrated clusters.

The optimized structures of the two lowest energy tautomers, N7H and N9H, of theophylline, at the MP2/6-311++G(d,p) level of theory are shown in Fig.1. The relative energies and the dipole moments of the two lowest energy tautomers using MP2, CC2 and DFT (employing various functionals) methods are summarized in Table S1 of the ESI. The corresponding structural parameters of these tautomers are listed in Table S2 of the ESI. As seen in Table S1 the lowest energy tautomer is the N7H form while the N9H tautomer is ~ 41 kJ/mole higher in energy at each level of theory. Theophylline has two carbonyl groups, C_2-O_{11} and C_6-O_{13}, joined to N_1 atom as shown in Figure 1 . At the MP2/6-311++G(d,p) level of theory the bond distance of C_6-O_{13} carbonyl of N7H tautomer, 1.227 A^0, is found slightly greater than that of C_2-O_{11} carbonyl, 1.224 A^0, while in N9H tautomer the C_6-O_{13} bond distance, 1.218, is found slightly lower than that of C_2-O_{11} bond distance,1.224. (See Table S2 of the ESI).Overall the difference in the bond lengths of the optimized geometries in two tautomers of bare theophylline were found to be less than 0.06 A^0. However significant changes were found in the bond angles N_9-C_4-C_5, C_4-C_5-N_7, C_5-N_7-C_8, C_8-N_9-C_4, N_9-C_8-H_{14}, C_4-C_5-C_6 and N_3-C_4-C_5 (See Table S2 of the ESI). The total electron density of theophylline indicates a build-up of charge density on the oxygen and nitrogen atoms and nodes at the other atoms. The NBO calculations at the MP2/6-311++G(d,p) level of theory led to negative charge densities of -0.729, -0.720, -0.623, 0.578, -0.574 and -0.599 in theophylline on O_{11}, O_{13}, N_1, N_3, N_7 and N_9 atoms respectively (See Table S 5 of the ESI). The negative charge densities on the nitrogen atoms are also large but not as significant as on the oxygen atoms. The other tautomer N9H led to negative charge densities of -0.731, -0.680, -0.633, 0.577, -0.461 and -0.633 on above atoms respectively at the same level of theory. One can note that there is an electronic charge displacement from O_{13} and N_7 atoms and accumulations of charges on the N_1 and N_9 atoms due to the tautomerisation of N7H into N9H form. Furthermore the computed dipole moment of the ground state N9H tautomer of 7.91 Debye is much larger than the dipole moment, 4.28 D, of N7H at the MP2/ 6-311++G(d,p) level of theory (See

Table S1 of ESI). Therefore it seems that the electronic charge displacement in the N9H tautomer causes a large separation between the effective charges forming the dipole.

We have computed the harmonic vibrational frequencies and intensities of the two theophylline tautomers. To the best of our knowledge, no detailed experimental vibrational spectra in isolated (or gas phase) theophylline have yet been published. Callahan et al[18] have investigated the gas phase vibrational spectra of theophylline using resonant two photon ionization and IR-UV double resonance spectroscopy but they could observe only one band at 3500 cm^{-1} and assigned that as a NH-stretching band of N7H tautomer. They have reported that the calculated frequencies of the N7H and N9H tautomers at B3LYP/6-311+G(2d,p) level are indistinguishable from each other, however it seems to be ambiguous. Balbuena et al [41] calculated the vibrational spectra of N7H tautomer of anhydrous theophylline at the B3PW91/6-311G level of theory. Present calculations at the B3LYP/6-311++G(2d,2p) level of theory predicts a difference of more than 12 cm^{-1} between NH stretching frequencies of the two tautomers (see Table 1). We have compared our results to experimental IR spectra observed in solution/condensed phase reported by Nolesco et al.[1] Harmonic vibrational frequencies computed at B3LYP/6-311++G(2d,2p) level (using the MP2/6-311++G(2d,2p) optimized geometry) have been shown to yield an excellent agreement[42] with the experimental data. [1,18] and there is no need of any further scaling in the most of vibrational fundamentals excluding for the NH stretch mode. In the experimental IR spectra[1] the carbonyl stretching modes consists of two major bands; the higher wavenumber band and the lower wavenumber band. Similar to caffeine [42,43] the two C=O groups of theophylline couple into an in phase C=O stretching vibration and an out of phase stretching vibrations. The out of phase $(C=O)_2$ stretching mode is observed at a lower frequency while the in-phase mode is observed at higher frequency.[10] Change in the harmonic wave numbers of NH and carbonyl stretching modes due to tautomerisations of theophylline were found to be significant, The harmonic wave numbers of selected stretching modes for the two lowest energy tautomers of theophylline are given in Table 1. The rotational constants and zero point vibrational energy of the two tautomers of theopylline are listed in supplementary Table S3. The values of rotational constants of the two tautomers yield similar values which show that they have similar mass distributions. The relative energies, rotational constants, dipole moments and harmonic frequencies of the two most stable tautomers remain for future experimental

verification. The structure and spectroscopic properties of theophylline and its analogous molecules [44,45] can be compared to our results.

3.2.Optimized geometries of monohydrated complexes of theophylline (N7H) monomer.

Similar to caffeine [42,43], theophylline possesses three main sites for hydration, into which a water molecule can bind strongly: (1) the C(6) carbonyl group (2) the C(2) carbonyl and (3) the N_9 atom. Figure 2 shows the optimized ground state structures of five lowest energy conformers of Thp_1-$(H_2O)_1$ clusters, two O_1-bonded (involving C_6=O carbonyl), two O_2-bonded (involving C_2=O carbonyl) and one N-bonded cluster. In each complex, the input geometry of the N7H tautomer of bare theophylline was used for the complexation with a water. As shown in Fig 2 these complexes are assigned as (I), (II), (III), (IV) and (V) isomers according to the order of their relative energies and stability. The relative and binding energies of Thp_1-$(H_2O)_1$ complexes at the various levels of theory are summarized in Table 2.We find that M06-2X method give energy value more near to MP2 in comparison to other DFT functionals and can perform much better for H-bonded systemss.[43] The binding energies with basis set superposition error correction of these Thp_1-$(H_2O)_1$ complexes, I, II, III, IV and V at the M06-2X/6-311++G(d,p) level of theory are found to be 60.57, 34.43, 30.48, 28.90 and 28.03 kJ/mole respectively (See Table 2). Similar trend of the order of stability is also found at X3LYP and wB97X-D levels. The isomer I of Thp_1-$(H_2O)_1$ in which both theophylline and water act as accepters as well as donors, was found much more stable than the other four isomers. The larger stabilization energy for this isomer I arises from the additional stability of the cyclic structure with two hydrogen bonds between water and the C6=O and N(7) H moiety, as illustrated in Fig 2. Therefore it is clear that at C(6) carbonyl site within a close proximity of the N(7)H position is the most favorable site for hydration in theophylline. Report on the structural investigations on theophylline complexes[46] indicated that the oxygen of C_6=O bond participates in the formation of very strong intermolecular hydrogen bonding. The structural parameters and dipole moments of these hydrated complexes at M06-2X/6-311++G(d,p) level are listed in Table S4 of ESI and Table 2 respectively. Due to the formation of a relatively strong hydrogen bond in the most stable isomer I of the Thp_1-$(H_2O)_1$ complex, the NH stretching fundamental (of the complex I) is red shifted significantly by 335 cm^{-1}. As mentioned in the earlier section 3.1 that the two

C=O groups in theophylline is coupled into an in-phase $(C=O)_2$ stretching vibration and an out of phase $(C=O)_2$ stretching vibration modes and the out of phase $(C=O)_2$ stretching mode is observed at a lower frequency than the in-phase mode.[42] It seems that the C_6-O_{13} carbonyl, stretching mode strongly mixes with the C=C stretching mode to give rise out of phase (lower frequency) C=O stretching band. It was reported that the valence bond electron delocalization through the central N_1 atom favors lower energy for the coupled out of phase $(C=O)_2$ stretching mode in caffeine.[43] Thus the out of phase $(C=O)_2$ stretching modes of the isomer I of the O_1-bonded Thp_1-$(H_2O)_1$ complex, is red shifted significantly (by 27 cm^{-1}) whereas the in-phase stretching mode shows a relatively small red shift (of 10 cm^{-1}). Thus we may expect that the interaction of water at C_6=O carbonyl site within a close proximity of the N(7)H has apparently an important stabilizing effect on the full structure of theophylline. The computed dipole moment of hydrated complex-I of theophylline decreases after the complexation, while the dipole moments of the other O-bonded complexes III and IV increases (See Table 2 and Table S4 of ESI). Interaction of water between the C_6=O carbonyl site and N_7H produces a decrease in the overall charge separation which results in unusual decrease in the dipole moment of the complex I.

3.3. Molecular geometries of theophylline dimers.

The ground state molecular geometry of anhydrous theophylline dimer Form IV, which has been optimized using MP2 and DFT (B3LYP and M06) methods, is presented in Fig. 3a. The calculated hydrogen bond lengths and bond angles along with the corresponding experimental data are listed in Table 3. The binding energy of the theophylline dimer IV with BSSE correction is found to be 21.04 , 20.48 and 19.94 kcal/mole at the MP2/6-311++G(d,p), M06/6-311++G(d,p) and B3LYP/6-311++G(d,p) levels of theory, respectively. The corresponding hydrogen bond distance H...O at MP2, M06 and B3LYP levels was found to be 1.7455, 1.7568 and 1.7596 Å respectively, which are in consonance to the experimental value obtained in solid phase.[11] It should be clear that MP2 and DFT calculations refers to the gas phase of anhydrous theophylline. The high binding energy of the dimer IV indicates the existence of strong hydrogen bonding between the theophylline monomers. It should be noted here that B3LYP and M06 perform well for the optimization of such a strongly H-bonded complex. Comparison of the dimer IV structure data with those

of the monomer reveals that the strong hydrogen bonding has pronounced effects on the geometry of the -C (O)-N(H)- segment of the molecule. Thus the N-H and C=O bond lengths increased to the extents of 0.019 and 0.016 and 0.0214 and 0.0140 Å from monomer at MP2/6-311++G (d, p) and M06/6-311++G (d, p) levels respectively The angular orientations of C=O and N-H also display significant changes (see Table 3). The N-H...O=C type hydrogen bond is one of the most frequently occurring bonds in the biological systems and nature of such HB was investigated.[47] It is worth mentioning that for N-H...O=C hydrogen bonds there are nice correlations between the magnitudes of the interaction energy components and the H…O distances.[48] In the isatin dimer [49] which also involves double N-H...O=C hydrogen bonds similar to the theophylline dimer IV, the hydrogen binding energy and H…O distance are found to be 15.52 kcal/mole and 1.855 Å respectively at the B3LYP/6-311++G(d,p) level of theory. The binding energy and the H…O distance for dimer IV at B3LYP/6-311++G (d,p) level are found to be 19.94 kcal/mole and 1.760 Å. Thus we can assume the decrease in H…O distance as an indicator of increasing strength of the hydrogen bond interaction energy. The natural atomic charges calculated by NBO method [25] are listed in Table S 5 of ESI, which shows a significant increase in negative charge densities at the hydrogen bonded oxygen atom upon dimerisation in Form IV. NBO results indicate that the lone pair and π bonding electrons of the C=O group play an important role in the donor-acceptor interaction as well as in the stronger H-bond formation for the dimer IV complex. Seton and Khamar [10-12] reported experimentally that the crystal structure of anhydrous form IV consists of dimers similar to those observed in hydrated theophylline (Form M). Therefore, the intermolecular interaction between theophylline dimer and water (at N_9 sites) was also studied at B3LYP/6-311++G(d,p) and M06/6-311++G(d,p) levels (see Fig 3b). Due to the interaction with water molecules at N_9 site the H…O distance in dimer IV decreases to 1.747 Å (See Fig 3b) and hydrogen binding energy (with BSSE correction) between monohydrated theophylline monomers increases to 21.15 kcal/mole at M06/6-311++G(d,p) level which shows that hydrogen bonding strength increases in the hydrated dimer IV and it is converted to monohydrate dimer Form M on contact with water. Similar results were also found at B3LYP/6-311++G(d,p) level. Thus we can conclude that further stability is being conferred to the hydrogen bonding of dimer Form IV after hydration, as experimentally reported by Khamer et al in solid phase. [12]

Theophylline dimer related to anhydrous Form II, which is connected by N-H…N and C-H…O hydrogen bonds, was proposed by Nolesco et al.[1] The geometry optimization of this dimer II (see Fig 2c) has been also performed at the M06/6-311++G (d, p) and B3LYP/6-311++G (d, p) levels of theory. The hydrogen bond geometry parameters are listed in Table 3. The binding energy of this dimer was found to be 10.91 kcal/mole at DFT-B3LYP which is about half that of the dimer Form IV. Similar results are found at DFT-M06 and MP2/6-31+G (d)} levels. The structural parameters of the theophylline dimers IV and II are given in Table S6 and S7 respectively of ESI. The rotational constants and zero point vibrational energy of the theophyllie dimer's are listed Table S8 of ESI, which remain for future experimental verification.

Thus we can conclude that the dimer IV is the most stable dimer of anhydrous theophylline in the gas phase. Our results supports the results obtained from the recent experimental crystal structure investigation[10-12] that the dimer arrangement of Form IV is likely to be more thermodynamically stable. Surprisingly, Callahan et al.[18] investigated the gas phase structure of theophylline using resonant two photon ionization and IR-UV double resonance spectroscopy, but they could not observe any theophylline dimer. A possible explanation for this observation is a faster excited state decay of the theophylline dimer enabled by an efficient internal conversion mechanism.

3.4. Computed Infrared spectra of theophylline dimers.

Computed IR spectra of theophylline monomer and dimer Form IV and II are shown in Fig 4. Experimental IR spectra of the theophylline crystals in different forms reported recently by Seton et al.[10] have been compared with the calculated values. The DFT-B3LYP values of Form IV, II & M at basis set 6-311++G(d,p) are found to be in better agreement with the experiment.[10] The calculated harmonic wave numbers are only slightly larger than the experimental values, excluding the hydrogen bonded XH-stretching modes. This disagreement for H-bonded stretching modes, may be partly due to the anharmonicity. Usually complex molecules are treated in the harmonic oscillator approximation, where only quadratic terms are included in the molecular potential energy function giving rise to independent vibrational normal modes. However, for hydrogen bonded systems, the higher order terms of the molecular potential energy function in every single vibrational

coordinate that lead to anharmonicity effects cannot be neglected. Hydrogen bonding enhances the anharmonicity of the PES resulting in strengthened mechanical coupling of different vibrational modes. It was reported that anharmonic contribution in the XH stretching modes in hydrogen bonded systems is significant and its magnitude is roughly inversely proportional to the bond distance.[50,51] For the O-H bond, the anharmonic contribution is largest whereas for N-H bond it is larger than that of C-H bonds.[47]Therefore in order to compensate the use of a harmonic oscillator approximation, we have scaled H-bonded OH and NH stretching vibrations by 0.932, 0.944 factors respectively; however the other modes were mainly scaled by 0.97 factor. Selected IR wave numbers of Form IV and II and their corresponding experimental values and vibrational assignments are listed in Table 4.

Region 4000-2000 cm^{-1}

Calculated frequencies and intensities of the vibrational fundamentals of this region agree well with the experiment (See Table-4).Experimental IR spectra of anhydrous theophylline Form IV reported by Seton et al.[10] reveals that the most intense band observed in this region at 3089 cm^{-1} is aroused due to hydrogen bonded NH-stretching vibrations. Due to significant hydrogen bonding in dimer IV, NH stretching vibrations coupled into each an in-phase $(NH)_2$ stretching vibration and an out-of-phase $(NH)_2$ stretching vibration and from a visual inspection of the mode it was clear that the band at 3089 cm^{-1} actually corresponds to out of phase H-bonded $(NH)_2$ stretching mode. The corresponding NH-stretching mode in the spectra of Form II was observed at 3058 cm^{-1} and has relatively very weak IR intensity.[10] Calculated NH-stretching IR peaks, shown in Fig 4, are found in consonance with the observed position and intensities of IR bands. Callhan et al.[18] observed the NH stretching vibration band at 3500 cm^{-1} in the IR-UV spectrum of theophylline monomer which is in agreement with the predicted NH stretching mode of theophylline monomer. This NH-stretching band is red shifted in the dimer form IV and form II by 411 and 442 cm^{-1} respectively. Here it should be interesting to note that inspite of moderate strong hydrogen bonding in dimer IV, the red shift of NH-stretching vibration in dimer II is slightly higher than dimer IV. This may have been aroused due to more elongation of the H- bonded NH bond in the Form II. Recently, Zwier and co-workers [52]

provided one example in which the conformer with the lowest NH-stretch has the strongest H-bonding. In the dimer form M (see Fig 3b) the hydrogen bonded O-H stretch, due to presence of water, was predicted at 3338 cm^{-1} which is in consonance with the experimental IR frequency reported by Seton et al.[10] However the O-H stretch frequency at 2908 cm^{-1} reported by same authors was not supported by our DFT calculations. DFT-B3LYP calculations of dimer form M, predicted that the H-bonded NH-stretching vibrations are coupled with CH stretching mode and the most strong band observed in the IR spectra of Form M at 3104 cm^{-1} [10] is assigned to out of phase $(NH)_2$ and $(CH)_2$ stretching mode vibrations. In the IR spectra of form IV[10] the weak intensity peak observed at the shoulder of NH-stretching band in the longer wavelength side (~3119 cm^{-1}) was attributed to CH-stretching whereas the band at 2991 cm^{-1} was assigned as symmetric CH_3 stretching mode. Finally by comparing the experimental IR wavenumbers with the calculated harmonic wavenumbers of form IV in this region, we can conclude that the magnitude of anharmonicity is significant in the H-bonded XH stretching modes and is found inversely proportional to the bond distance, as reported earlier. [50]

Region 2000-1000 cm^{-1}

DFT calculations employing both B3LYP and M06 functional predicted intermolecular coupling between carbonyl stretching vibrations of dimer IV. The two $(C=O)_2$ groups couple into in-phase $(C=O)_2$ stretching vibration and out-of-phase $(C=O)_2$ stretching vibration. Intensity of intermolecular in-phase carbonyl stretching vibrations is predicted to be very weak in comparison to that of out-of-phase carbonyl vibrations. Both carbonyl stretching bands observed at 1703 and 1632 cm^{-1} in the experimental IR spectra of dimer IV is found consistent with calculated DFT frequencies (See Fig 4 and Table 4). In the lower frequency mode each of the pair of $(C=O)_2$ stretching vibration is out of phase with a slight dominance of hydrogen bonded pair. In the higher frequency mode the carbonyl stretching vibrations in each of theophylline molecules are in phase, however each pair (H-bonded and free carbonyls) is out of phase with the dominance of free pair of $(C=O)_2$. The intensity of lower frequency $(C=O)_2$ stretching mode, which corresponds to the most intense (and broad) IR band of Form IV (observed at 1632 cm^{-1}), is predicted triple to that of higher frequency mode (See Fig 4), which is found consistent with the observed IR

intensity.[10] Predicted red shift in the lower frequency mode due to the hydrogen bonding, ~34 cm^{-1}, is found in consonance to the observed experimental shift.[10]

In contrast to the NH-stretching mode, N-H in plane bending mode of the Form IV undergoes blue shift upon hydrogen bonding [See Table 4]. The intense triplet bands observed at 1439, 1414 and 1394 cm^{-1} in the IR of Form IV is ascribed to the symmetric CH_3 bending vibrations.

Many researchers including Nolasco et al.[1] recently, reported three carbonyl stretching peaks in the IR and Raman spectra of anhydrous form II. However, they assigned middle peak pertaining to metastable form III which seems to be ambiguous. Calculated frequencies of dimer Form II predicted four carbonyl modes at the three frequencies (See Fig-2) as reported earlier for the isatin dimer.[46] Therefore the middle observed carbonyl stretch peak reported by Nolasco et al [1] can be pertaining to Form II and does not belong to metastable form III. It was noticed that DFT calculations ascribed intramolecular coupling between carbonyl stretching vibrations in dimer II which is not similar to that found in dimer IV.

Region below 1000 cm^{-1}

The most intense IR bands of the dimer form IV observed in this region at 744 and 759 cm^{-1} are attributed to carbonyl wagging (out of plane bending) vibrations and the bands at 980 and 790 cm^{-1} are ascribed to CH_3 rocking vibrations. The intense IR band observed at 601 cm^{-1} was ascribed to CH- wagging vibration. The IR band at 816 cm^{-1} is expected due to coupled NH and CH wagging vibration. In the dimer form II carbonyl wagging vibrations were observed at 742 and 762 cm^{-1} whereas CH_3 rocking vibrations were observed at 977 and 785 cm^{-1} .

3.5. Vertical Electronic Excitation Energies.

The absorption spectra of methylated xanthine derivatives measured in water and acetonitrile solutions have two clear band systems in addition to a weak broad band at the shoulder of the high energy band.[19] The observed low energy band of theophylline is located approximately between 4.28 - 4.86 eV, whereas the weak shoulder band is located between 5.34 -5.58 eV.[19] The electronic absorption spectrum computed in the present

work at B3LYP-TDDFT/6-311++G(d,p) level is in remarkable agreement with the experiment concerning both positions and intensities of absorptions. Table 5 shows the TDDFT vertical excitation energies of the low lying singlet excited states of (anhydrous) theophylline monomer and dimer Form IV calculated at B3LYP-optimized S_0 geometries. The VEE for the theophylline monomer computed by second order approximate coupled cluster (CC2) method is also included in Table 5. The lowest-lying vertical singlet-singlet transition of theophylline monomer, leading to the $^1\pi\pi^*$ state, is computed at 4.60 eV, with an oscillator strength 0.14. This excitation energy is found consistent with the lower energy broad absorption band of anhydrous theophylline, observed at 4.56 and 4.58 eV in acetonitrile and aqueous solution respectively.[19] The highest occupied molecular orbital (HOMO) of theophylline is a π-orbital. Its electron density is expected to localized mainly on the C_4-C_5 fragment. The photoelectron spectra and NBO calculations also show that the HOMO in theophylline molecule is formed mainly from $\pi_{C4\text{-}C5}$ bonding orbital, similar to caffeine.[43] The lowest excited $^1\pi\pi^*$ state is dominated by single configuration corresponding to HOMO → LUMO (0.69) excitation. The energy gap between HOMO and LUMO of the theophylline was found to be 4.46 eV at B3LYP/6-311++G(d,p). The optimized geometry at the DFT-D3(B97-D)/TZVP level of theory shows relatively lower H-L gap of 3.56 eV which seems to be ambiguous. The lowest excited $^1\pi\pi^*$ state geometry of theophylline was optimized at B3LYP/6-311++G(d,p) and DFT-PBEO/TZVP levels and the 0-0 band transition energies computed at 4.09 and 4.295 eV respectively. The dipole moment, 2.27 D, of the S_1 state is predicted to be lower than that of the ground state dipole moment, 3.50 D, at the B3LYP/6-311++G(d,p) level of theory, which indicates that position of S_0-S_1 band may be blue-shifted in polar solvents. Recently observed electronic absorption spectra of theophylline[9] revealed a blue shift of ~ 1 nm upon changing solvent from acetonitrile to water.

The second transition, leading to $^1n\pi^*$ state, is computed at 4.98 eV, with zero oscillator strength. This S_0-S_2 ($^1n\pi^*$) transition is expected to involve the excitation from the lone pairs at carbonyl oxygen atoms and N_9 atom. The S_o-S_2 transition of relatively weaker intensity seems to be unresolved and hidden near the first absorption peak at 4.56 eV (~272 nm). The weaker intensity of this transition was predicted due to a small Franck-Condon factor resulting from rather poor overlap of potential surfaces.[18] The third absorption peak

observed as a shoulder near 5.42 eV, is another $^1\pi\pi^*$ excitation energy and corresponds to S_o-S_3 and S_o-S_4 transitions. The most strong electronic absorption peak of theophylline,[19] is associated with a number of transitions computed at 5.97 and 6.39 eV with high oscillator strengths and is attributed to $^1\pi\pi^*$ state (See Table 5). This strong absorption peak was observed in caffeine at ~ 5.95-6.12 eV,[43] which may belongs to Platt's ^1B_b and ^1B_a states.[43] The lowest lying excited states of all the five isomers of monohydrated theophylline were investigated by TDDFT method[35-36] in order to estimate the spectral shift caused by micro-hydration as well as by macro-hydration. The TDDFT (B3LYP) vertical excitation energies (VEE) to the lowest excited S_1 ($^1\pi\pi^*$) state, for Thp_1-$(H2O)_1$ complexes show that the lowest S_1 ($^1\pi\pi^*$) state for the O_1-bonded clusters (I and IV) involving C(6) carbonyl are red shifted by 188 and 417 cm^{-1} respectively. The VEE to the same state for N-bonded cluster is also red shifted by 408 cm^{-1}. The electronic frequency shift measures the difference in binding energy of the complex in the S_0 and S_1 states.[53] So in the case of complexes I and IV, the π-π^* electronic excitation increases the strengths of H-bonds to water. The $S_0(\pi)$ -$S_1(\pi^*)$ transitions for the isomers II and III of Thp_1-$(H2O)_1$ are blue shifted from corresponding monomer transitions by 387 and 564 cm^{-1}, respectively. Thus the blue shift in complexes II and III reflects a decrease in the binding energy upon electronic excitation by 387 and 564 cm^{-1}, respectively. The effect of hydration on S_1($^1\pi\pi^*$) excited state due to bulk water environment, mimicked by the polarizable continuum model (PCM)[37-38] and conductor like screening model (COSMO),[39] both show a small blue shift in accordance with the result of experimental electronic absorption spectra in aqueous solution.[19] The corresponding VEE to S_2 ($^1n\pi^*$) state for each O-bonded Thp_1-$(H2O)_1$ complexes were blue shifted.

Interestingly, the computed VEE for the lowest lying singlet excited states of dimer IV, corresponding to the lowest lying bright $^1\pi\pi^*$ state of monomer, lie at 4.46 and 4.65 eV, which shows both red and blue spectral shift respectively of the optically bright state of theophylline upon dimerization. Since the absorption spectra of theophylline have a low energy broad band starting at~ 4.28 eV extends up to ~4.86 eV. This indicates that the broader nature of the low energy band, which is peaked at 4.56 eV (which is average transition energy of the transitions at 4.46 and 4.65 eV) may be aroused due to presence of dimer Form IV in solid/liquid sample of theophylline.

4. Conclusion

Present work reported the five lowest energy Thp_1-$(H_2O)_1$ clusters at the M06-2X/6-311++G(d,p) levels of theory for the first time. The isomer I (O_1-B) of Thp_1-$(H_2O)_1$ in which both theophylline and water act as accepters as well as donors, was found about two times more stable than the other four isomers. Due to formation of relatively strong hydrogen bond the NH stretching mode of the most stable complex I, is red shifted significantly by 335 cm^{-1}. The out of phase $(C=O)_2$ stretching mode of this complex is also red shifted (> 25 cm^{-1}) whereas the in-phase stretching mode shows a relatively small red shift. The optimized structure, interaction energy and IR and electronic spectra of newly characterized anhydrous theophylline dimer Form IV, computed for the first time by MP2 and DFT (M06 and B3LYP) methods employing the 6-311++ G(d,p) basis set. The binding energy of newly characterized dimer Form IV is found about double of the dimer related to Form II, considered as the most stable form during the 70-year history of theophylline usage. Inspite of the methylation, theophylline dimer Form IV, involving C(6)=O carbonyl in H-bond interaction, had a strong hydrogen bonded structure. It has been determined that further stability is being conferred to the N-H…O=C hydrogen bonding of the dimer IV with interaction of water molecule at N_9 sites. Dimerization induced changes in transition vibrational frequencies and intensities have been determined which is found consistent with the experimental results. The intensity of lower frequency $(C=O)_2$ stretching mode which corresponds to the most intense IR band of Form IV at 1632 cm^{-1} is predicted triple to that of higher frequency mode. Anharmonicity in the hydrogen bonded XH stretching modes of dimer Form IV is found significant, which is approximately inverse of the bond length. The B3LYP-TDDFT vertical electronic excitation energies for the theophylline monomer is found in consonance to the experiment. The lowest excited $^1\pi\pi^*$ state is dominated by single configuration corresponding to HOMO → LUMO (0.69) excitation. The effect of hydration on $S_1(^1\pi\pi^*)$ excited state mimicked by COSMO bulk water environment show a blue shift in accordance with the result of experimental electronic absorption spectra in aqueous solution. The VEE corresponding to the lowest singlet excited $\pi\pi^*$ state is shifted both towards low and high energy side upon forming dimer IV. The computed vibrational mode

frequencies as well as the VEE of the neutral theophylline and its hydrated and dimeric complexes provide the characteristic 'spectroscopic signatures' which can reflect differences in the nature of hydrogen-bonded interactions in different complexes.

Acknowledgement.
The research was supported by Department (Ministry) of Science and Technology, (DST) Government of India, New Delhi by the research project ref. no. SR/S2/LOP-16/2008.Author is grateful to Mr Santosh Kumar Srivastava, JRF of the above DST research project for the assistance in the preparation of Figures and Tables of the manuscript.

Supporting Information Available:

The computed structural parameters, rotational constants, total energies/binding energies of theophylline monomer/dimer and monohydrated complex at MP2/6-311++G(d,p)/ M06/6-311++G(d,p)/ levels are submitted here as a supplementary information, which is available in the online version of the paper.

References

1. M. M. Nolasco, A. M. Amado, P. J. A. Ribeiro-Claro,
Chem. Phys. Chem., 2006, **7**, 2150-2161.
2. E. Suzuki, K.Shimomura, K. Sekiguchi, *Chem. Pharm. Bull.,* 1989**, 37**, 493-497.
3. Y.Ebisuzaki, P. D.Boyle, J. A. Smith, *Acta Cryst. C*, 1997, **53**, 777-779.
4. K.Matsuo, M. Matsuoka, *Cryst. Growth Des*. 2007, **7**, 411-415.
5. H.J.Zhu, C.M. Yuen, D.J. Grant, W. *Int. J. Pharm.*, 1996, **135**, 151-160.
6. N. V.Phadnis, R. Suryanarayanan, *J. Pharm. Sci.*, 1997, **86**, 1256-1263.
7. E.D.L.Smith, R.B.Hammond, M.J.Jones, K. J. Roberts, J. B.O. Mitchell,
S. L.Price, R. K.Harris, D. C.Apperley, J. C.Cherryman, R.Docherty,
J. Phys. Chem. B , 2001,**105**, 5818-5826.
8. Y. Ebisuzaki, P.D.Boyle and J. A. Smith, *Acta Crystallogr.* 1997, **C53**, 777-779.
9. A. M. Amado, M. M. Nolasco, P. J. A. Rebeiro-Claro,
Journal of Pharmaceutical Sciences 2007, **96**, 1366-1379.
10. L. Seton, D. Khammer, I. J. Bradshaw, G.A. Hutcheon,
Cryst. Growth Des. 2010, **10**, 3879-3886.

11. D. Khammer, R.G. Pritchard, I. J. Bradshaw, G.AHutcheon, L. Seton,
Acta Cryst. C, 2011, **67**, 496-499.
12. D.Khammer, I.J.Bradshaw, G.A.Hutcheon, L.Seton,
Cryst. Growth Des.**,** 2012, **12**, 109-118.
13. G.R. Desraju, *Nat. Mat.* (2002) , **1** , 77-79.
14. C. E.Crespo-Hernandez; B.Cohen; P.M.Hare and B.Kohler,
Chem. Rev., 2004, **104** , 1977-2020.
15. M.P. Callahan, B.Crews, A.Abo-Riziq, L. Grace, M. S.de Varies, Z.Gengeliczki,
T. M.Holmes,and G.A. Hill , *Phys. Chem. Chem. Phys.,* 2007, **9**, 4587-4591.
16. S. Yamazaki, A.L. Sobolewski and W. Domcke,
Phys. Chem. Chem. Phys., 2009, **11**, 10165-10174.
17. D.Nachtigallova, A.J.A. Aquino, S.Horn & H. Lischka,
Photochem. Photobiol. Sci., 2013, **12**, 1496-1508
18. M.P. Callahan, Z.Gengeliczki, N. Svadlenak, H.Valdes, M.S de Varies
and P.Hobza, *Phys. Chem. Chem. Phys.* 2008, **10**, 2819-2826.
19. J. Chen and B.Kohler, *Phys. Chem. Chem. Phys.,* 2012, **14,** 10677-10682.
20. C.Moller, M.S.Plesset, *Phys. Rev.*,1934, **46,** 618-622.
21. C.Hattig, and F. Weigned,. *J.Chem. Phys.* 2000**, 113**, 5154.
22. A.D. Becke, *Phys. Rev.* A, 1988, **38,** 3098-3100.
23. C.Lee, W. Yang,; R.G. Parr, *Phys. Rev.* B, 1988, **37,** 785-789.
24. A.D. Becke, *J. Chem. Phys.* 1993, **98,** 5648-5652.
25. M.J. Frisch et al, Gaussian 09, Revision A.02, Gaussian, Inc., (Wallinford CT, 2009).

26. TURBOMOLE V6.4; Turbomole Gmbh: (Karlsruhe,Germany,2012).
27. J. P. Perdew and Y. Wang, *Phys. Rev. B,* 1992, **45**, 13244 -13249.
28. X.Xu, and W. A. Goddard III**,** *PNAS,* 2004, **9,** 2673-2677.
29. Y.Zhao and D.G. Truhlar, *Ther. Chem.Acc.* 2008, **120**,215-241.
30. E. G. Hohenstein, T. C. Samual, C.D. Sherrill., *J.Chem. Theory Comput.* 2008,**4**, 1996- 2000.
31. J. D. Chai, M. H. Gordon, *Phys. Chem. Chem. Phys.* 2008, **10**, 6615.
32. G. Grimme, J. Antony, S. Ehrlich, H. A Krieg, *J. Chem. Phys.* 2010, **132**, 154104.
33. R.A. Marta, R.Wu, K.R.Eldridge, J.K. Martens, T.B. McMohan, *Phys.Chem.Chem.Phys.***,** 2010, **12**, 3431-3442.
34. S.F.Boys, F. Bernardi, *Mol. Phys.* 1970, **19** , 553-566.
35. E. Runge and E.K.U. Gross, *Phys. Rev. Lett.* 1984, **52,** 997-1000.
36. A. charaf-Eddin, A.Planchat, B.Mennucci, C.Adamo and D.Jacquemin, *J.Chem. Theory Comput.* 2013,**9**, 2749-2760.
37. D. Jacquemin, S. Chibani, B.Le Guennic and B. Mennucci, *J.Phys.Chem. A* 2014, **118**, 5343-5348.
38. D. Mafti, G. Zbancioc, I.Humelnicu and I.Mangalagiu, *J.Phys.Chem. A* 2013, **117,** 3165-3175
39. A. Klamt and G. Schüürmann, *J. Chem. Soc. Perkin Trans*., 1993, **2** , 79
40. J.P.Perdew, M. Ernzerhof, K.Burke, *J. Chem. Phys.* 1996, **105,** 9982-9985.
41. D. Balbuena, Perla B.; W.Blocker, R.M. Dudek, F.A. Cabrales-Navarro, P. Hirunsit, *J. Phys. Chem. A* 2008, **112**, 10210-10219
42. S. K. Srivastava and V. B. Singh , *Spectrochim. Acta A,* 2013, **115,** 45-50.
43. V. B. Singh, *RSC.Adv.,*2014,**4**,58116-58126.
44. C. Parkanyi, C. Boniface, J-J Aaron, M. Bulaceanu-MacNair, M. Dakkouri, Collect. Czech. Chem. Commun. 200), **67**, 1109-1124.
45. M. Karthika, R. Kanakaraju, L. Senthilkumar, *J. Mol. Model.* (2013), **19**, 1835-1851.
46. S. Tarulli and E.J. Baran, *J. Raman Spectroscopy* 1993, **24**, 139-141.
47. Y. Matsumoto, Jun-ichi Iwamoto and K. Honma, *Phys. Chem. Chem. Phys.,* 2012, **14,** 10677-10682.
48. R.G. Gora, S.J. Grabowski, J. Leszczynski, *J. Phys.Chem.A* 2005, **109**, 6397-6405.
49. V. B. Singh, M. K.Singh, A. Gupta, *J.Mol. Struct. THEOCHEM*, 2009, **909**, 483-485.

50. S. Limpijumnong, *Materials Research Society Symposium Proceedings*, 2004, **813**, 119-130.
51. J. Dreyer, J. *Chem. Phys.,* 2005, **122,** 18306.
52. W.H. James III, E.E.Baquero, V.A. Shubert, S.H. Choi, S.H.Gellman, T.S. Zwier, *J. Am. Chem. Soc.,* 2009, **131**, 6574-6590.
53. T.A.LeGreve, W.H.James III and T.S. Zwier, *J. Phys. Chem. A.,* 2009, **113**, 399-410.

Table 1 Selected ground state vibrational stretching frequencies (cm^{-1}) and IR intensity with vibrational assignments of two stable tautomers of theophylline

Approximate description of vibrations	Calculated values at B3LYP/6-311++G(2d,2p) level		Experimental frequencies of N(7)H form[1] (cm^{-1})
	Tautomer N(7)H	Tautomer N(9)H	
NH str.	3501* (112)	3514* (66)	3501[+]
CH_3 str. (+) at N_1	3037 (26)	3035 (27)	3032
CH_3 str. (+) at N_3	3030 (28)	3029 (32)	3032
$(C=O)_2$ sym. str.	1718 (439)	1737 (407)	1713
$(C=O)_2$ asym. str.	1676 (888)	1684 (838)	1665
C=C str.	1604 (65)	1628 (115)	1608
(C=N + C=C) str.	1579 (119)	1542 (176)	1565

Abbreviations used: (+), in phase; (-), out of phase, str. stretching.*NH str. is scaled by 0.976.[+] Value correspond to ref(18)

Table 2 Relative electronic energies (kJ/mol), dipole moments (Debye) in parenthesis and binding energies (kJ/mol) of the lowest energy conformers of monohydrated theophylline (Tph_1-$(H2O)_1$) calculated by DFT-X3LYP, wB97XD and M06-2X methods employing the 6-311++G(d,p) basis set.

Tph_1-$(H2O)_1$ complexes	E^{X3LYP}	E^{wB97xD}	E^{M06-2X}	B. E^{X3LYP}	B. E^{wB97XD}	B. E^{M06-2X}
I	0.0 (2.592)	0.0 (2.650)	0.0 (2.741)	61.39	61.35	60.57
II	29.88 (3.733)	29.73 (3.762)	28.24 (3.428)	33.19	31.30	34.43
III	31.34 (5.502)	31.03 (5.451)	29.59 (5.132)	31.70	29.73	30.48
IV	33.27 (5.566)	33.08 (5.802)	31.70 (5.691)	30.98	29.39	28.90
V	32.37 (4.033)	- -	33.41 (4.366)	25.37	-	28.03

Table 3
Hydrogen bond Geometries of Theophylline Form IV, II and M

Dimer Form	Structural Parameters/ (Å), (°)	Experimental Values [a]	B3LYP/ 6-311++G(d,p)	M06/ 6-311++G(d,p)	MP2/ 6-311++G(d,p)
Anhydrous Theophylline **Form IV**	N_{20}…O_{13}	2.759	2.778 -	2.777 -	2.763 -
	N_{7}…O_{26}	2.736	2.778 -	2.777 -	2.763 -
	NH...O_{13}	1.80	1.760 - -	1.757 - -	1.746 - -
	NH...O_{26}	1.80	1.760 - -	1.757 - -	1.746 - -
	N_{20}-H	0.98	1.0305 -	1.0314 -	1.0309 -
	N_{7}-H	0.97	1.0305 -	1.0314 -	1.0309 -
	N_{26}-H…O_{13} (°)	168	169.0 -	169.4 -	168.4 -
	N_{7}-H…O_{26} (°)	163	169.0 -	169.4 -	168.4 -
Hydrated Theophylline **Form M**	N_{20}…O_{13}	-	2.767	2.769	-
	NH...O_{13}	-	1.747	1.747	-
	N_{20}-H	-	1.0315	1.0320	-
	N_{26}-H…O_{13} (°)	-	169.2	170.2	-
Anhydrous Theophylline **Form II**	N_{20}…N_{9}	-	2.952 2.944*	2.920 -	-
	NH... N_{9}	-	1.925 1.916*	1.892 -	-
	N_{20}-H	-	1.0313 1.0324*	1.0336 -	- -
	N_{20}-H…N_{9}	-	173.9 173.7*	172.6 -	- -

[a] **experimental values are taken from ref. [11]**

Table 4 Computed IR wave numbers (cm^{-1}) and intensities of theophylline dimer's

Theoretical and Experimental IR Wave Numbers (cm^{-1}) and Intensities of Theophylline Dimer IV, II, and M						Approximate description of vibration
Experimental Values[10]	Form IV Calculated value at B3LYP/6-311++G(d,p) Level		Experimental Values[10]	Form II Calculated value at B3LYP/6-311++G(d,p) Level		
Wave Number (Intensity)	Wave Numbers	IR Int.	Wave Number (Intensity)	Wave Numbers	IR Int.	
3341[M](s)	3348[M]	1541[M]				[M]OH str. (H-bonded)
3119 (m)	3125	39	3119(s)	3120	55	CH str.(-)
3089 (vs)	3090	4033	3058(s)	3055	2068	NH-str. (-) H-bonded
2991(m)	2973	71		CH_3 str. (+)		CH_3 str. (+)
1702(s)	1701	915	1707(s)	1709	458	[IV] $(C=O)_2$ Str.(-) in dimer; $(C=O)_2$ str. (+) in each monomer; Free $(C=O)_2$ vibration dominates. [II] $(C=O)_2$ Str. (+) in one molecule involving free $(C=O)_2$ pair of dimer.
-	1697	0.0	-	1698	467	[IV]$(C=O)_2$ Str. (+) in dimer as well as in each monomer [II] $(C=O)_2$ Str. (+) in a molecule of dimer involving H-bonded C=O
1632(vvs)	1638	2748	1680(s)	1671	887	[IV] $(C=O)_2$ Str.(-) in dimer as well as in each monomer. [II] $(C=O)_2$ Str. (-) in one molecule involving free $(C=O)_2$ pair of dimer.
-	1634	0.0	1660(s)	1651	1195	[IV] $(C=O)_2$ Str.(+) in dimer; $(C=O)_2$ str. (-) in each monomer; H-bonded $(C=O)_2$ vibration dominates. [II] $(C=O)_2$ Str. (-) in a molecule of dimer involving H-bonded C=O
-	1569	150	Overlapped	1591	48	C=C str.
1548(s)	1541	416	1560(vs)	1548	160	NH bend ; CN Str.
1438(s)	1440	200	1440(s)	1425	123	Sym CH_3 Str.
1414(s)	1410	133	-	-	-	Sym CH_3 Str.
1394(s)	1393	239	-	-	-	Sym CH_3 Str.
1162(s)	1162	42	-	-	-	NH & CH Scissoring
744(s)	742	40	-	737	19	C=O deformation

Intensity: w-weak,m-medium ,s-stron,vs-very strong, vvs-very very strong, (+)-in phase, (-)-out of phase.
[M] Correspond to hydrated theophylline dimer Form M; [IV]correspond to dimer Form IV; [II]correspond to dimer Form II,[*] Experimental values values taken from Reference 10.

Table 5 Vertical excitation energies (eV) and oscillator strengths (in bracket) of the anhydrous theophylline monomer and dimer Form IV

State	Energy of observed absorption Peaks (in eV)	Calculated Values at TDDFT-B3LYP/6-311++G(d,p) level			Calculated values of monomer at CC2/6-311++G(d,p) level
		Isolated Monomer	Monomer in COSMO Bulk Water	Isolated Dimer Form IV	
$^1\pi\pi^*$	4.54 (~4.40-4.80)	**4.603** (0.146)	**4.607** (0.202)	**4.457** (0.161) **4.651** (0.164)	**4.737** (0.152)
$^1n\pi^*$	-	4.871 (0.000)	5.185 (0.000)	5.202 (0.0) 5.204 (0.0)	**4.982** (0.0)
$^1\pi\pi^*$	-	5.172 (0.002)	5.417 (0.002)	5.372 (0.0) 5.420 (0.006)	**5.133** (0.0)
$^1\pi\pi^*$	5.39 (~ 5.34-5.58)	5.618 (0.016)	5.618 (0.011)	5.615 (0.078) 5.639 (0.0)	**5.604** (0.014)
$^1\pi\pi^*$	-	5.974 (0.128)	5.975 (0.292)	-	**-**
$^1\pi\pi^*$	-	6.385 (0.340)	6.306 (0.261)	-	**-**

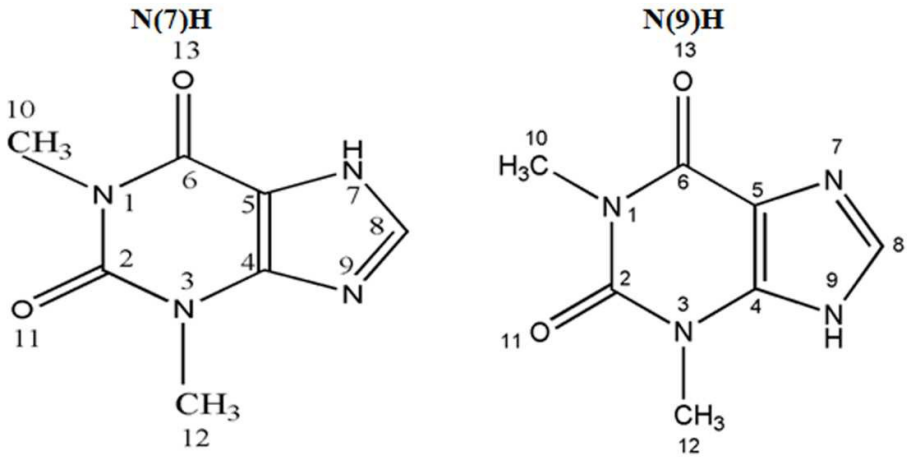

Fig. 1(a) Chemical structures of theophylline tautomers.

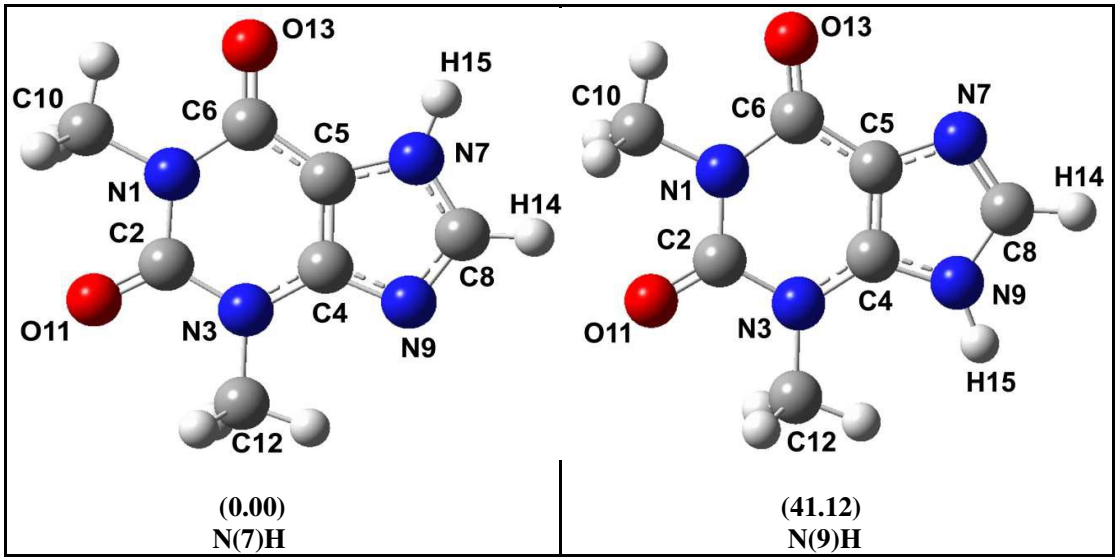

Fig. 1(b) Optimized structures and relative energies (kJ/mol) of the two most stable tautomers of neutral theophylline at MP2/6-311++G(d,p) level.

Conformer	Tph_1-$(H_2O)_1$ (I)	Tph_1-$(H_2O)_1$ (II)	Tph_1-$(H_2O)_1$ (III)	Tph_1-$(H_2O)_1$ (IV)	Tph_1-$(H_2O)_1$ (V)
Relative energy (kJ/mol)	**0.00**	**28.24**	**29.59**	**31.70**	**33.41**
Structure	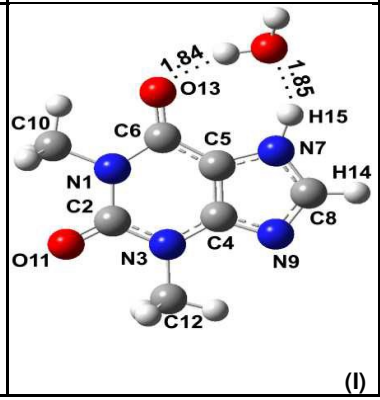	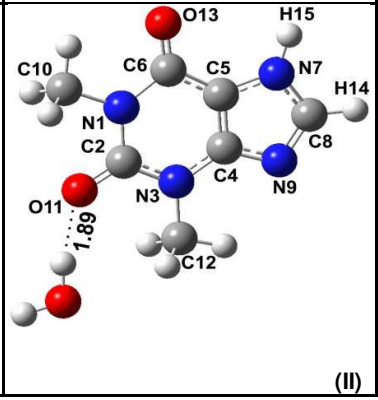	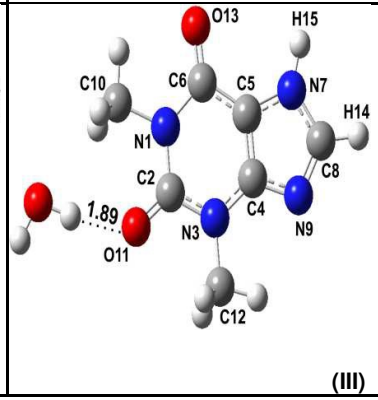	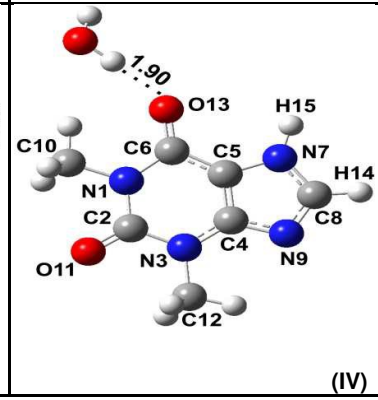	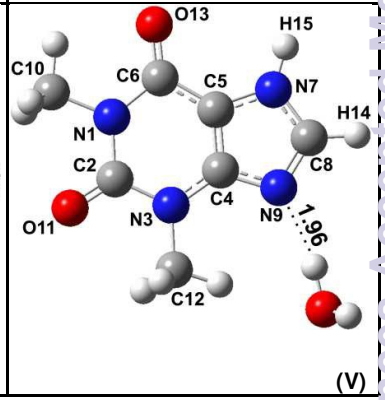

Fig. 2 Computed optimized geometries and relative energies of theophylline monohydrates {Tph_1-$(H_2O)_1$} at M06-2X/6-311++G(d,p) level.

(a)

(b)

(c)

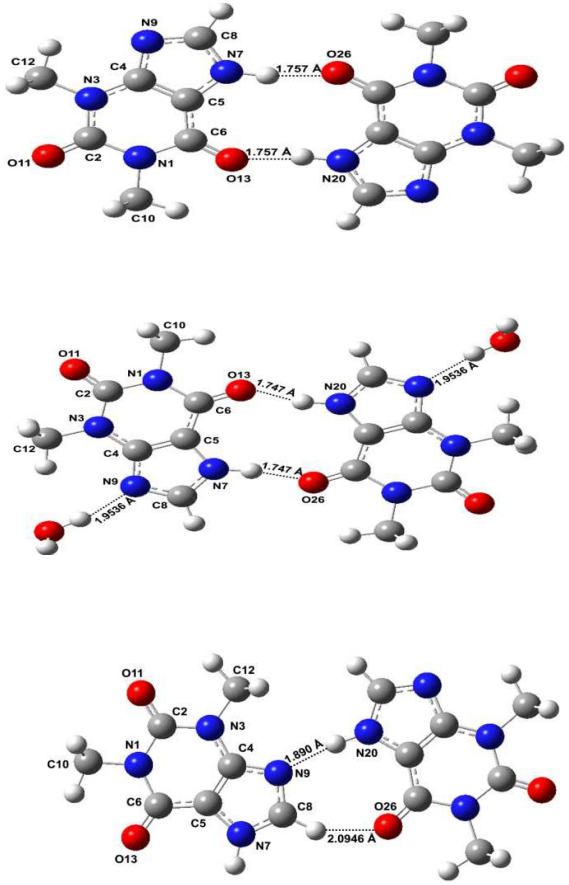

Figure 3. Computed optimized Geometries of **(a)** Theophylline dimer Form IV **(b)** Monohydrated Theophylline dimer Form M **(c)** Theophylline dimer related with Form II at M06/6-311++G (d,p) Level.

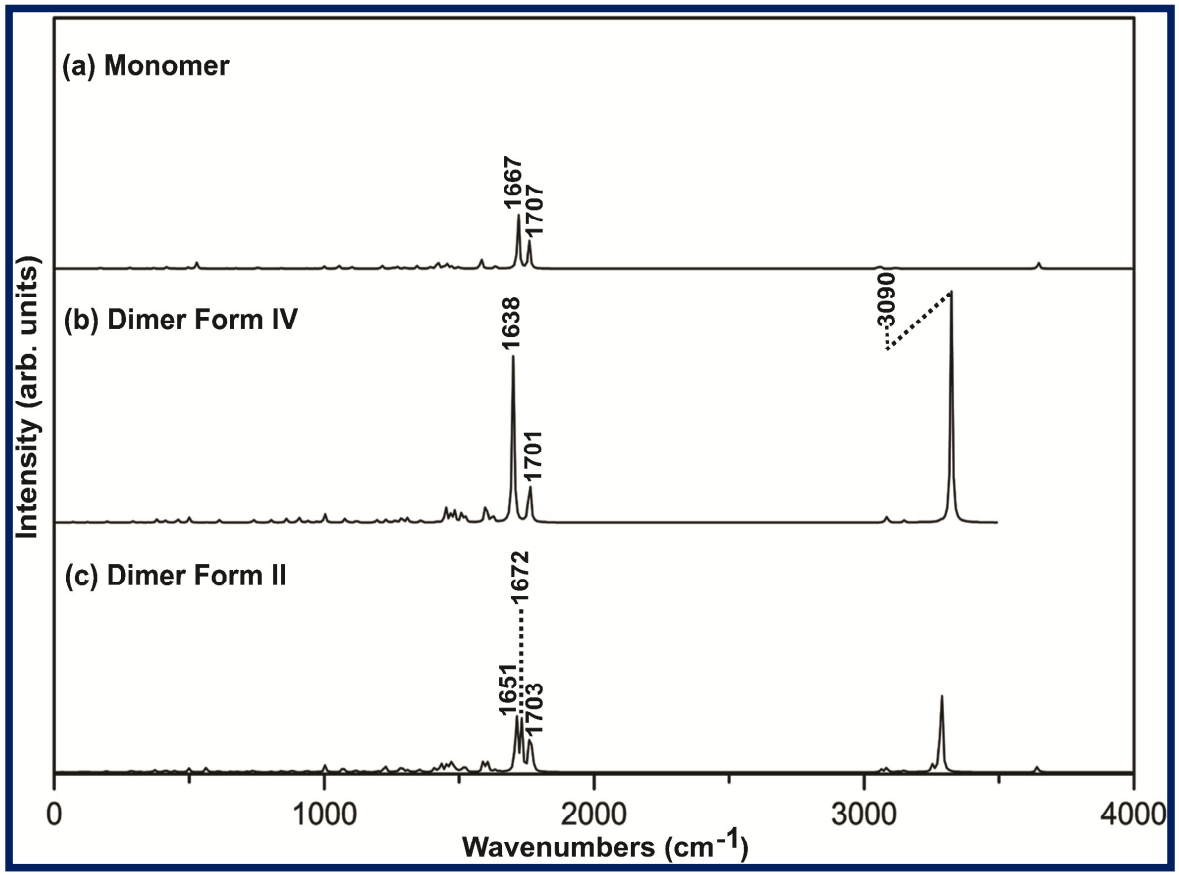

Figure 4. IR spectra of anhydrous theophylline monomer and dimers IV and II at B3LYP/6-311++G(d,p) level